Atmospheric Environment Vol. 18, No. I I, pp. 2541–2551, 1984
Printed in Great Britain.

0004–6981/84 $3.00 + 0.00
© 1984 Pergamon Press Ltd.

ABSORPTION CHARACTERISTICS OF FOREST FIRE PARTICULATE MATTER

E. M. PATTERSON
School of Geophysical Sciences, Georgia Institute of Technology, Atlanta, GA 30332, U.S.A.

C. K. MCMAHON
USDA Forest Service, Southeastern Forest Experiment Station, Southern Forest Fire Laboratory, Dry Branch, GA 31020, U.S.A.

(First received 27 January 1984 and in final form 21 *May* 1984)

Abstract-Absorption properties of smokes from laboratory fires that represent prescription hums in the Southern states have been quantified to relate variations in measured absorption parameters to variation in fire conditions and to estimate emission factors for elemental'carbon. Results showed significant differences in absorption of the smoke emissions between flaming and smoldering combustion with specific absorption coefficient B_a values ranging from 0.04 $m^2 g^{-1}$ for smoldering combustion to 1 $m^2 g^{-1}$ at 632.8 nm for flaming combustion. These measured optical properties and previously measured size data were used in Mie calculations to determine the overall radiative properties for the smokes from these fires. Mie calculations for $\lambda = 550$ nm indicate that, somewhat less than 50% of the extinction will be due to particulate matter absorption in flaming combustion, whereas only about 5 % of the extinction will be due to absorption under purely smoldering conditions. Calculated mass concentration/scattering (C_m/σ_S) ratios for $\lambda = 500$ nm show only a slight variation with n_{IM}, decreasing from 3.3 x 10^5 $\mu g m^{-2}$ at an imaginary refractive index (n_{IM}) = 0.07 to avalueof 2.7 x 10^5 $\mu g m^{-2}$ at n_{IM} = 0.007. The ratios calculated for the low absorption cases are generally consistent with previous experimental observations, although these calculations suggest that some of the variations seen in this ratio are consistent with variation due to differences in the optical properties of the particulates.

Key *word index:* Absorption, aerosol absorption, optical properties, visibility, smoke properties, aerosol readiative effects, forest fires, particulate matter,

INTRODUCTION

One obvious environmental effect of the smoke plume from a wildland fire is reduced visibility. This visibility reduction can occur within the plume itself either immediately downwind of the fire with visibility reduced to a few meters, causing health and safety hazards, or at much greater distances from the fire where the plume contributes to a psychological perception of reduced air quality. Later, after the plume has lost its identity, the smoke can still significantly contribute to regional pollution hazes.

Because there are economic and environmental effects associated with such visibility reductions, there is a need to be able to predict the magnitude of reduction resulting from wildfire and prescribed burns. This visibility reduction is due to the presence of particulate matter (from 0.01 to 10 μm in size) which scatters and absorbs light. The amount of visibility reduction depends on the amount of material emitted as well as on the optical properties of the material which affect scattering, absorption, and total extinction. The visual range is related to the particle extinction coefficient, σ_E, by the Koschmeider (1924) relation $V = 3.9/\sigma_E$. σ_E is the sum of the scattering coefficient σ_S and the absorption coefficient σ_A.

When absorption is an appreciable fraction of total extinction, the particle absorption can have a significant contribution to visibility reduction; in addition, highly absorbing aerosols can have an effect on perceived contrast levels (Middleton, 1952; Roessler and Faxvog, 1981) and thus on human perception of color and the visual impact of pollution that can be quite different from that of nonabsorbing aerosols.

The relative importance of absorption for carbonaceous aerosols resulting from combustion can be quite variable. σ_A/σ_E ratios $\approx$ 0.85 have been measured under laboratory conditions for soots containing large amounts of elemental carbon (Patterson and Marshall, 1982); by comparison, absorption measurements of the benzene soluble organic fractions of an urban aerosol (Patterson, 1979) indicate σ_A/σ_E ratios of less than 0.1 at $\lambda = 0.55$ μm. There is considerable evidence that much of the absorption of carbonaceous materials is due to elemental or 'graphitic' carbon (Weiss et al., 1976; Rosen et *al.*, 1978), while the volatile or extractable organic material is relatively nonabsorbing. The measured absorption will depend on the relative amounts of each material present.

Wildland fires can be quite variable and the smoke from them is a complex mixture of organic and inorganic materials. Hence, the particulate fraction of these smokes is highly variable both in physical

properties and in chemical composition (McMahon, 1983). Most particles in the smokes are formed from gaseous organic compounds produced by pyrolysis and combustion. Nucleation, condensation, and coagulation form both liquid and solid particles. Liquid particles can range from the highly volatile and short lived to long lived, tarry, viscous spherical particles. Solid particles can also be spherical; more commonly they assume other forms, including chain-like aggregates that are characteristic of soot (Russell, 1979).

The composition of smoke depends on the nature of the fuel (Sandberg et al., 1978) as well as on the type, intensity and phase of the fire (Ryan and McMahon, 1976). Various components of smoke are generated from four phases of thermal decomposition in the burning process of forest fuels (McMahon, 1983). In the pre-ignition phase, moisture is evolved and fuel pyrolysis begins; in the flaming phase, gases evolved from pyrolysis combust; in the smoldering phase, combustion proceeds without a visible flame; and in the final glowing phase, solid surface oxidation predominates after all volatile materials have been evolved. The relative importance of these phases will depend on the type of fire (whether a heading or backing fire) and the amount of fuels consumed. A heading fire moves rapidly with the wind whereas a backing fire moves slowly into the wind.

Measurements of laboratory burns of pine needles taken by McMahon and Tsoukalas (1978) show that heading fires produce higher total particulate matter emissions than backing fires and that their smoldering phase produces much higher emissions than the flaming phase. Furthermore, the benzene soluble organic fraction, an indication of total organic component of smoke, is significantly higher in the smoldering phase than in the flaming phase, and is generally higher than in backing fires.

When collected on glass fiber filters, particulate matter from forest heading fires ranges in color from yellow to dark brown to black. These different colors reflect the composition of the smoke; in particular, dhey point to differences in the relative amount of elemental carbon present and to significant differences in the absorption parameters for the smokes horn these fires.

The primary purpose of this study was to quantify the absorption properties of smokes from laboratory fires that simulate prescribed burning of forest litter fuels. Our primary measurement procedure was the diffuse transmission technique described by Patterson and Marshall (1982) and by Patterson et al. (1982). Diffuse reflectance measurements, using techniques described by Patterson et al. (1977), and solution transmission measurements were also made for a more detailed investigation of the absorption properties of selected samples.

We have also sought to determine emission factors for the particles and for the elemental carbon for these fires. In addition, we have used measured optical properties and previously measured size data to determine the overall radiative properties for the smokes from these fires.

EXPERIMENTAL PROCEDURES

Combustion experiment

A series of experimental fires were conducted at the Southern Forest Fire Laboratory in Macon, GA. These laboratory tires consisted of 30 fires using slash pine needles as fuel, 2 fires using palmetto mixed with pine needles, as well as several preliminary test fires using pine needle fuel designed to check our sampling procedure.

Slash pine needle litter was chosen because it is one of the fuel types involved in prescription burning in the Southeast, is well suited for laboratory burning methods, and has been thoroughly studied.

To investigate the variation in absorption that might. be encountered in prescribed tires and to relate this variation to fires and fuel conditions, the pine needle fire experiments were performed for a range ofconditions to represent thevariation expected for natural-cases. Three important factors affecting the types and amount of smoke produced are fuel loading, fuel moisture, and fire slope. A positive or upslope fire simulates a heading fire and a negative or downslope fire simulates a backing fire.

The pine needle burns consisted of a two-level factorial design with three. factors (moisture, loading, slope) replicated at each level and with fourcenter-point experiments to test for curvature (Table 1).

Two exploratory burns to investigate the effect of a live fuel type on absorption properties of particulate matter emissions were conducted with the palmetto fuel mixed with pine needles. The palmetto fuel is representative of live understory fuels burned in the Southeast. On the basis of field observa-

Table 1. Pine needle experimental burns for each; fire series, by design factor and total emission factors of fires

Variable	Backing (downslope) fire series				Heading (upslope) fire series				Centerpoint (zeroslope) fires
	01	02	03	04	05	06	07	08	09
Replications	3	3	2	2	2	3	3	4	4
Moisture level (%)	4	20	4	20	4	20	4	20	12
Fuel loading ($kg\,m^{-2}$)	0.5	0.5	2.4	2.4	0.5	0.5	2.4	2.4	1.5
Slope (%)	-50	-50	-50	-50	+50	+50	+50	+50	0
C_m (g)	10.65	7.10	21.5	22.6	7.65	7.08	116.2	154.5	22.2
EF_{TSP} ($g\,kg^{-1}$)	21.3	13.7	8.3	8.8	15.3	13.6	45.5	60.9	14.5
C_e (g)	1.48	1.21	2.82	2.04	1.43	1.02	2.79	3.39	2.45
B_a ($m^2\,g^{-1}$)	.93	1.15	0.88	0.65	1.26	1.26	0.98	0.16	0.73

tions, we expected this fuel to result in a smoke with a relatively high soot content.

The combustion experiments were carried out on a, 1 x 1.2 m burn table in-the combustion room of the laboratory (Fig. 1). Correlative measurements of fuel weight, total air flow, and gaseous emissions were also made during the fire to aid in the interpretation of our particulate measurements and to allow the calculation of total emission factors of these, fires. Details of the fuel bed preparation and combustion room operation have been reported by McMahon and Tsoukaks (1978).

Particulate matter sampling

All emissions from the combustion experiments were channeled through a large stack for sequential monitoring of particulate matter. Samples were collected by two systems: a modified high-volume sampler using a Type A glass fiber filter

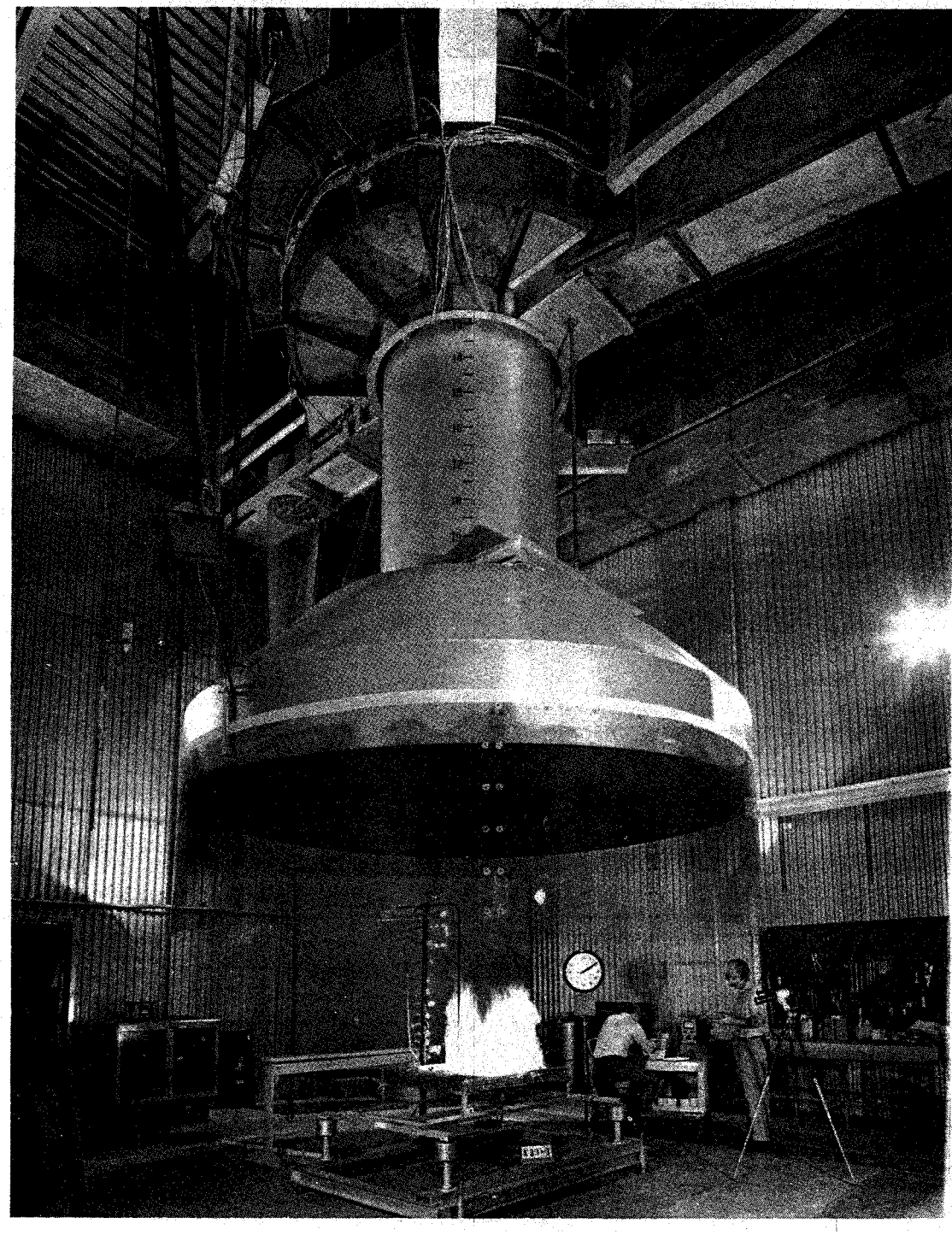

Fig. 1. Southern Forest Fire Laboratory Combustion Room. Slope of burn table can be adjusted to alter burning conditions.

and a low-volume sampler using 47-mm diameter Pallflex QAST quartz fiber filters. Mass loadings were determined by gravimetric analysis for both the low- and the high-volume filters. Absorption was measured by means of diffuse transmission techniques using the 47-mm quartz fiber filters. Several 47-mmfilter samples were collected during each fire to determine differences in the emissions between the flaming, transition and smoldering combustion stages. The sampling periods for the fires were chosen to correspond as closely as possible to the different phases of the fires. For the backing fires (Series 01-04) there were.two sampling periods for each fire. One began 30 s after ignition (to avoid ignition effects on the particulate matter emissions) and encompassed the time required for the fire to spread to the end of the fuel bed. The second sampling period began at the end of the first period and continued until the end of the fire.

The bum characteristics of the heading fires (Series 05–08) lead to a greater differentiation into flaming and smoldering components. To map out these differences, more than two sampling periods per fire were generally used. The first sampling period, as before, included the time from 30 s after ignition until the flame had reached the end of the fuel bed; the emissions during this first period were characteristic of the flaming phase. The second period extended from the end of the first period until there was no flame visible; this period was a transition period in which both smoldering and flaming combustion were important. Following this transition period, there were one or more periods that were dominated by smoldering combustion. Because of the rapid fire spread during Series 05, the sampling during this series was begun at ignition in order to obtain sufficient sample material.

Temperatures at the filter surface were monitored. Because of the large volume of cool dilution air moving through the stack, temperatures were kept below 65°C. Flow through the samplers approximated isokinetic conditions, and since the smoke particles are known to be below 5 μm dia., the collected sample appears to be representative of the fire emissions.

Samples for diffuse reflectance measurements were also collected onto 20 x 25 cm, 0.4 μm pore size Nuclepore filters during a laboratory heading fire in which there was agcod separation into smoldering and flaming phases. These diffuse reflectance samples were collected for both the flaming and the smoldering phases.

Absorption measurement procedures

Diffuse transmission technique. *The* experimental apparatus for our diffuse transmission measurements consisted of a He-Ne laser (λ = 632.8 mm), the 47-mm diameter filter whose transmission was measured, an acrylic plastic diffuser, and a photomultiplier detector. In our procedures, the transmission of a blank filter (Ii) and of a loaded filter (Ii) are measured and the quantity τ is determined from the equation

$$\frac{I_i^1}{I_1} - e^{-\tau}. \qquad (1)$$

The aerosol volume absorption coefficient σ_A is then calculated from the equation $\tau = \sigma_A x$, where x, the path length of air swept out by the filter, is determined from the volume of air sampled through the filter and the known area of the filter. The calculations assume that the scattered light reaching the detector is the same for both loaded and blank filters and that the attenuation of the light is due only to the optical absorption.

Measurements were made from quartz fiber filters which show an enhanced response relative to the actual absorption, so an empirically determined correction factor 3.3 (Patterson and Marshall, 1982) was applied to our attenuation data. Other similar relative response determinations have 'been reported by Nolan (1977) and by Sadler *et al.* (1981).

The overall accuracy of thediffuse transmission technique has been estimated at $\approx$ 20% by Weiss et *al.* (1979). Comparison of this method with in-situ spectrophone measurements of a highly absorbing aerosol (Szkarlat and Japar, 1981) leads to a similar estimate of uncertainty. For aerosols with low absorption, the- uncertainty will be somewhat greater. We estimate that the uncertainty in our absorption measurements, including the uncertainty in our empirical correction factor, is $\approx$ 35-40 %; a more complete discussion of our procedure is given in Patterson and Marshall (1982).

Bulk absorption parameters such as the specific absorption coefficient B_a and the imaginary component of the refractive index n_{IM} may also be determined from the corrected attenuation data if the amount of material on the filter is known. B_a is defined by the equation

$$B_a = \frac{\tau A}{m}, \qquad (2)$$

for transmission spectroscopy with m the mass of material in the beam, A the cross-sectionalarea of the beam subtended by the absorbing 'material and τ the measured optical depth. B_a has dimensians of area/mass; in this study the units for B_a are $m^2\ g^{-1}$ If the absorber is nonscattering, then the above definition is equivalent to

$$B_a = \frac{k}{\rho} \qquad (3)$$

with k the Lambert absorption coefficient of the bulk material and ρ the bulk density. For an aerosol, an analogous definition can be made with

$$B_a = \frac{\sigma_A}{C_m}, \qquad (4)$$

where C_m is the mass concentration of the aerosol suspension.

If the assumption is made that all of the absorption is due to elemental carbon (C,) then a measured value of B_a for elemental carbon, together with the measured absorption can be used in equation (4) to determine the C_e concentration in theaerosol. Such determinations have been made in this study using B_a data of Szkarlat and Japar (1981), corrected for the difference in wavelength between their data and ours.

For a non-scattering solid, n_{IM}, the imaginary component of the refractive index is related to k by the equation

$$n_{IM} = \frac{k\lambda}{4\pi}, \qquad (5)$$

with I the wavelength of an incident light. For anaerosol that consists of particles that are small relative to the wavelength of the incident light, Hänel and Dlngi (1977) have shown that n_{IM} may be determined from the approximate relation

$$n_{IM} = \frac{\lambda\rho}{12\pi}\frac{\sigma_A}{C_m}(n_{RE}^2 + 2), \qquad (6)$$

with n_{RE} the real component of the refractive index. Equivalently n_{IM} may be written in terms of B_a as

$$n_{IM} = \frac{\lambda}{12\pi} B_a (n_{RE}^2 + 2). \qquad (7)$$

Equations (6) and (7), however, have reduced accuracy for particles in the size range of aged smoke particles. Ratios of particle absorption to mass calculated as a function of size for particles in the size range of these smoke aerosols (see, e.g., Bergstrom, 1979) suggest somewhat lower n_{IM} values for a given B_a than do Equations (6) and (7); and matching of average calculated ratios to the observed B_a values provides an empirical estimate of n_{IM}

In this study, B_a and σ_a are directly measured quantities, which are used to determine n_{IM} values. These n_{IM} values must be considered more uncertain as discussed above because of possible variation in the density of the various components of the particle emissions (McMahon, 1983) as well as the approximations involved in deriving n_{IM} values.

Diffuse reflectance/solution transmission techniques. The polycarbonate filter samples for diffuse reflectance measurements were placed in spectral grade methylene chloride, which dissolved the polycarbonate filters as well as a portion

of the aerosol sample, and the undissolved aerosol was separated from the dissolved material by centrifugation. Following repeated washing with solvent, the excess solvent was evaporated to obtain the pure undissolved aerosol material. This preparation separates the smoke material into a methylene chloride soluble fraction and a methylene chloride insoluble fraction.

The absorption of the insoluble fraction was measured by diffuse reflectance techniques using the dilution method described by Patterson et al. (1977), in which the total diffuse reflectance of a mixture of aerosol and white standard is measured using an integrating sphere. Absorption properties, B_a and n_{IM}, are then determined from the known reflectance of the standard, the previously measured scattering properties of the standard, and the known concentration of aerosols in the mixture. Absorption of the soluble fraction of the sample was measured by standard solution transmission techniques.

RESULTS AND DISCUSSION

Wavelength dependent measurements of the absorption of the methylene chloride insoluble and the methylene chloride soluble fractions of smoke from well separate phases of a pine needle fire (in terms of the specific absorption B_a), are shown in Fig. 2(a) (flaming phase) and Fig. 2(b) (smoldering phase). The B_a values expected for elemental 'graphitic' carbon are also shown for comparison with our particulate matter measurements.

It is apparent from the figures that the absorption measured for the methylene chloride soluble fraction is quite similar for both flaming and smoldering combustion. This soluble fraction absorption is similar to the absorption of the benzene soluble organic fraction of an urban aerosol measured previously by Patterson (1979). Since the methylene chloride soluble fraction is analogous to the more commonly determined benzene soluble fraction, such similarity is not surprising. Somewhat surprisingly, measurements of the methylene chloride insoluble fraction show significant differences between flaming and the smoldering combustion. As expected, the flaming phase shows the strong influence of the elemental carbon component but the smoldering phase shows much less absorption, indicating that elemental carbon represents only a small portion of this insoluble fraction. The remainder of this fraction apparently consists of low absorption organic material that is not soluble in methylene chloride.

The relative importance of the two fractions varied with the combustion phase. During flaming combustion the methylene chloride soluble fraction represented approximately 44 % of the total sample mass, while during smoldering the soluble fraction increased to ~ 90 % of the total sample mass. By comparison, data of McMahon and Tsoukalas (1978) indicate that the benzene soluble organic fraction ranges from ~ 54% during flaming combustion to ~ 67 % during smoldering combustion.

The soluble and insoluble mass fractions were used to calculate mass weighted average B_a values for both the flaming and the smoldering phases. The

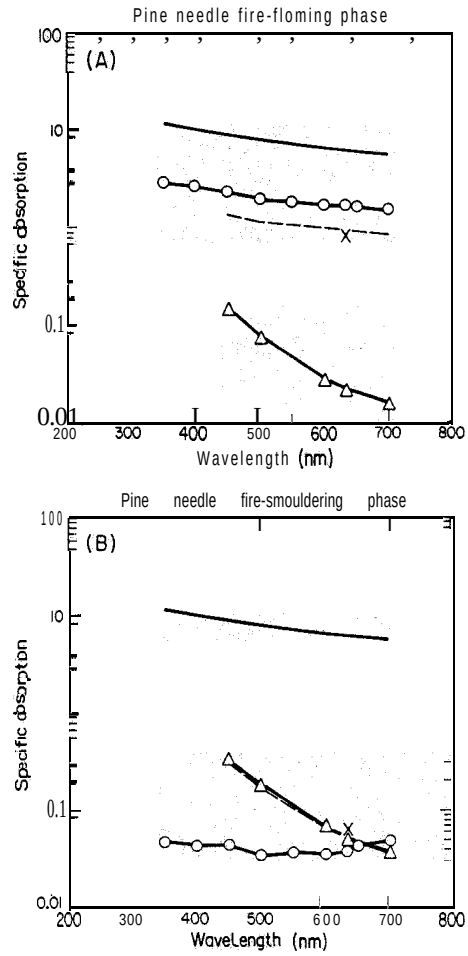

Fig. 2. Specific absorption values of smoke emissions for pine needle fire: (A) flaming phase; (B) smoldering phase: A- A- A, B_a values determined on methylene soluble component by solution transmission measurements; o-o-o, data on remaining material determined by diffuse reflectance; ------, mass weighted average B_a values; ——, B_a expected for pure elemental carbon and ×, measurement at 633 nm for a comparable sample using diffuse transmission techniques.

average B_a calculated for the flaming combustion is approximately 1 with a weak wavelength dependence; the average B_a for the smoldering combustion is much less, with a strong wavelength dependence that is similar to that of the methylene chloride soluble fraction. These average values are also shown in Figs 2(a) and (b).

These differences in calculated particulate matter absorption for the two phases account for the observed differences in filter appearances that were discussed in the introduction. The highly absorbing particulate matter from flaming combustion with its weak wavelength dependence will result in a dark grey or black filter. Smoldering phase emissions, by comparison, are characterized by much lower values of absorption at mid-visible wavelengths, with a strong wavelength dependence. These characteristics will cause filter samples collected during smoldering combustion to

have a brown to yellow appearance. Filters collected in a manner that includes both the flaming and smoldering components will be dark brown with intermediate absorption values.

Representative values of B_a determined by diffuse transmission techniques for $\lambda = 632.8$ nm are also shown for both flaming and smoldering phases. There do not appear to be major differences in the B_a's calculated by these techniques, and so our further, discussions of the results of our parametric study will be in terms of the diffuse transmission measurements for $\lambda = 632.8$ nm only.

A total of nine separate cases for different values of fuel loading, moisture, and slope were used in our pine needle absorption study. These cases and the corresponding fire conditions are shown in Table 1. Filter data were used to determine mass concentrations, absorptions coefficients, and specific absorption4 for each sampling period of the individual fires.

These measured absorption coefficients and mass concentrations for the individual fires were combined to calculate averages for each phase. The measured filter data and the known total combustion flow during each sampling period were then used to calculate total particulate matter mass emission and B_a values for each period and for the total fire. Under the assumption that the absorption is due entirely to elemental carbon whose B_a values are given in Fig. 2, we used our measured B_a values to calculate the elemental carbon mass emitted during each period and during the complete fire. Summary data on C_e and total particulate matter emissions and B_a values for the fires in each series are given in Table 1. Data for the individual periods in each of these series are given in Table 2. More complete data are available in Patterson and McMahon (1983).

The highest average B_a value measured was 2.4 for the flaming phase (PI) of series 05; most of the flaming phase values were clustered near 1 with the lowest flaming values ($\sim$ 0.7) measured during series 07. Each of these heading fire series shows a decrease in B_a after the initial flaming phase, with changes of filter appearance that correspond to the changes in B_a. The two fire series with the most clearly delineated separation into flaming and smoldering phases (07 and 08) were the heading fires with high fuel loading. These fires also showed the greatest differentiation in measured B_a values with the B_a values decreasing from $\sim$ 1 in the flaming phase to $\sim$ 0.2 in the transition period to $\sim$ 0.04 in the smoldering phase. The appearance of the filters for these fires changed from black for the flaming phase to gray-brown for the transition period to light brown for the smoldering phase. Although there were two sampling periods during the smolder-

Table 2. Elemental carbon, mass concentration, and absorption coefficients of particulate matter emissions for each fire series, by combustion phase

Fire series and combustion phase	Sampling period	3	C_m (g)	B_a ($m^2 g^{-1}$)
01				
Flaming	P1	0.99	8.22	0.81
Flaming	P2	6.49	2.43	1.35
02				
Flaming	P1	0.63	4.08	1.05
Flaming	P2	0.58	3.02	1.28
03				
Flaming	P1	1.60	12.05	0.94
Flaming	P2	1.13	9.48	0.80
04				
Flaming	P1	0.91	3.50	1.75
Transition	P2	1.13	19.10	0.45
05				
Flaming	P1	0.68	1.95	2.36
Flaming	P2	0.68	4.67	0.95
Transition	P3	0.09	1.03	0.58
06				
Incomplete data	—	—	—	—
07				
Flaming	P1	1.21	12.18	0.67
Transition	P2	1.28	51.58	0.17
Smoldering	P3	0.25	44.93	0.04
Smoldering	P4	0.05	7.53	0.04
08				
Flaming	P1	0.88	4.83	1.22
Transition	P2	1.87	63.52	0.20
Smoldering	P3	0.54	75.46	0.05
Smoldering	P4	0.10	10.66	0.07
09				
Flaming	P1	1.48	11.38	0.88
Transition	P2	0.97	10.79	0.61

Transition = mixed flaming and smoldering phases.

ing phase for these two series, no decrease in B_a was seen between the first and the second of these smoldering periods.

Analysis of the variation in B_a (Table 1) in terms of the variation in the experimental parameters (Box et al., 1978) shows that there was a significant dependence (95% level) on both the fuel loading and the slope (heading or backing), but not on the moisture. Physically, these data simply reflect the relative importance of flaming and of smoldering combustion. A heavy fuel loading tends to enhance the relative importance of the smoldering phase and the effect, is dramatically increased in the heading fires relative to the backing fires. Moisture differences (at least at the levels measured here) have little effect on B_a.

We may conveniently separate the data into two groups, shown in Table 3, one in which flaming combustion was predominant with B_a values near 1 and the other, consisting of series 07 and 08, in which smoldering combustion was dominant with the B_a values near 0.16. The C_e values are determined from the B_a values as described above.

Table 3. Simplified pine-needle study results by combustion phase

Combustion conditions	B_a, $m^2 g^{-1}$	C_e (%)
Flaming predominates	0.98	15
Smoldering predominates	0.16	2.5

Live fuel absorption study

Only two live fuel fires were conducted, each with a horizontal fuel bed. No attempt was made to investigate differences between heading and backing fires,, although we would expect that the fires with 0° slope would have burn characteristics intermediate between those of the heading and backing fires. The sampling protocol followed for these live fuel fires was that followed for the heading fires with three sampling, periods. Measured B_a values decreased from 0.68 $m^2 g^{-1}$ in the flaming phase to 0.24 $m^2 g^{-1}$ in the smoldering phase. An overall B_a of 0.44 $m^2 g^{-1}$ was measured for the total fire. This B_a value is intermediate between the pine needle heading and backing values. It is also significantly lower, however, than the 0° slope pine needle fires, suggesting that these measured palmetto live fuel emissions may have lower characteristic B_a values than comparable pine needle fuel fires. Additional studies would be necessary to fully evaluate the effect of burning live foliage on B_a values. Live foliage can contain up to 20% extractable hydrocarbons (terpenes, oils, resins, etc.) which are known to be more favorable soot-precursors than the highly oxygenated lignin and cellulose polymers found in woody fuels. Heavy black smoke has been observed during flaming combustion where live vegetation was a major component of the fuel burned.

Total particulate matter emissions factors (EF_{TSP}) for the pine needle fires are shown in Table 1. The 'alternate' high-volume sampling data were somewhat lower but consistent with these 47-mm sampler primary measurements. The emission factors data obtained during this study are consistent with earlier data reported for laboratory backing and heading fires (Ward *et al.*, 1976; McMahon and Tsoukalas, 1978). C_e emission data inferred from the absorption data are shown in Tables 1, 2 and 3. As a comparison with our optically inferred data, organic and elemental carbon mass loadings for selected filters were determined by thermal-optical techniques at the Oregon Graduate Center in Beaverton, Oregon (Johnson et al., 1981). Filter loading data for the Oregon Graduate Center elemental and organic carbon data and for the elemental carbon and total mass determined at Georgia Institute of Technology in Atlanta, Georgia, and the Southern Forest Fire Laboratory in Macon, Georgia, are shown in Table 4.

The Georgia Tech data indicate somewhat lower values of C_e than the Oregon Graduate Center data. However, the differences in relative graphitic carbon concentrations, between flaming and smoldering combustion are clearly seen in each data set. The organic carbon component of the mass ranges from 41 to 61%. The limits of this range represent the differences between flaming and smoldering combustion. If we look at the organic carbon as a percentage of total organic mass (determined by subtracting the elemental

Table 4. Total mass organic carbon and graphitic carbon for selected filter samples

Sample period and combustion phase	Total mass loading* (mg)	Organic carbont (%)	Graphitic carbont (%)	Graphitic carbon‡ (%)
010 P1 Flaming	2.11	50	20	12
010 P2 Flaming	0.64	45	27	20
071 P1 Flaming	3.92	41	33	8.4
071 P2 Transition	4.29	56	4.4	2.1
071 P3 Smoldering	3.76	61	1.6	0.5
071 P4 Smoldering	0.87	58	1.0	0.5

*Southern Forest Fire Laboratory data.
† Oregon Graduate Center data.
‡ Georgia Tech data.

carbon mass from the total sample mass), we see that the organic carbon represents a relatively constant percentage ($\sim 60\%$) of total organic mass.

Radiative properties of fire emissions

σ_E, σ_A, σ_S and other radiative properties of interest for these emissions may be determined by means of Mie scattering routines, using measured values of sizes and refractive indices. These calculations were made for four cases: one representative of flaming combustion corresponding to our measured B_a value of 1 $m^2 g^{-1}$, one representative of smoldering dominated combustion corresponding to our measured B_a of $0.16 m^2 g^{-1}$, one representative of smoldering only with a measured B_a of $0.04 m^2 g^{-1}$, and one corresponding to a $\lambda = 632.8$ B_a value of $0.50 m^2 g^{-1}$. This last case will correspond in a general way to the live fuel case as well as to our center point pine needle case. As such, we can consider that it is a representative of 'general' fire conditions for medium to low intensity fires in which both flaming and smoldering are important.

Particle size distributions were not measured during this series of fires; size distributions were measured, however, in an earlier series of comparable labortory fires. These earlier measurements have been reported by Ryan and McMahon (1976). For our calculations, we used a log normal approximation to their high concentration size distribution. A single size distribution was used for each of the four cases. This distribution should be valid for both flaming and smoldering combustion in low intensity fires such as our laboratory fires or prescribed burns in which the mechanical generation of large particles is not important. For our calculations, we have normalized these particle size distributions to a volume concentration of $500 \mu m^3 cm^{-3}$, a value comparable to those measured by Stith *et al.* (1981) in prescribed bum plumes in the Pacific Northwest. We have assumed a particle density (p) of 1.3 g cm- ^{3} for all cases. Our assumed density is based on data of Foster, although other data show values of approximately. 2 g cm- ^{3} (Radke *et al.*, 1983, and data of Stith *et al.*, 1981, discussed by Radke). For our assumed $\rho = 1.3 g cm^{-3}$, this volume concentration corresponds to a mass concentration of $650 \mu g m^{-3}$.

One n_{RE} value, 1.53, as measured by Foster (1959) was used for all of these radiative property calculations. n_{IM} values were determined from the measured B_a values for each of the cases.

Since one of the major interests of this study is the impact of these wildland fires on visibility, the radiative calculations were made for the mid-visible wavelength of 550nm rather than the 632.8 nm wavelength at which our measurements were made. We first used the wavelength dependence of the individual fractions shown in Fig. 2 to convert our 632.8 nm B_a values to values appropriate to 550 nm. These 550nm B_a values are 1.1, 0.22 and 0.08 $m^2 g^{-1}$ for the three pine needle cases and $0.6 m^2 g^{-1}$ for the 'general' case. The n_{IM} values were then calculated from these B_a values using (7) as well as the empirical matching of the calculated and the observed B_a values. The assumed particle density in all cases is 1.3 g cm^{-3}. n_{IM} values of calculated using Equation (7) are 0.1 for B_a = 1.1 $m^2 g^{-1}$, 0.018 for B_a = *0.22* $m^2 g^{-1}$, 0.0066 for B_a = *0.08* $m^2 g^{-1}$ and 0.05 for B_a = *0.6* $m^2 g^{-1}$. Comparable values calculated using the empirical matching are 0.07, 0.011, 0.004 and 0.03. We have used these empirical n_{IM} values in our further radiative calculations.

These calculated values for n_{IM} may be compared with previous measurements of the absorption characteristics of wood combustion particulate matter emissions reported by Foster (1959) for burning wood dust and by Nolan (1977, 1979) for a laboratory analogue of a slash burn. Nolan's data implies a B_a value of $1.7 m^2 g^{-1}$ 530 at nm for flaming combustion. Calculation of n_{IM} from this B_a using (7) results in a 530nm n_{IM} value of 0.13, a value quite comparable to ours. Both Nolan's and Foster's smoldering combustion values. of n_{IM} are significantly lower than ours: $n_{IM} = 4 \times 10^{-4}$ at 530nm reported by Nolan and $n_{IM} = 9 \times 10^{-4}$ at 550 nm for Foster's data, compared with our value of 6.6×10^{-3} at 550nm. We cannot say definitely why these differences exist, but there do appear to be different wavelength dependences in the data sets, suggesting differences in the chemical nature of the smoke in our measurements relative to these previous studies. The reasons for such possible differences ate not known, but may be related to the different fuels and to different conditions of the

Table 5. Calculated radiative properties for particulate emissions at $\lambda = 550$ nm

Combustion phase	" I M	$\sigma_E (m^{-1})$	$\sigma_S (m^{-1})$	ω
Flaming	0.07	2.46×10^{-3}	1.62×10^{-3}	0.66
Transition	0.011	2.01×10^{-3}	1.86×10^{-3}	0.93
Smoldering	0.004	1.95×10^{-3}	1.90×10^{-3}	0.97
'General' Case	0.03	2.16×10^{-3}	1.77×10^{-3}	0.82

Properties are calculated assuming a log normal size distribution with mean radius, $r_g = 0.045$ μm, standard deviation, $\sigma = 1.75$, and total particle number $N_p = 3.21 \times 10^5 cm^{-1}$, normalized to a total particulate volume of $500 \mu m^3 cm^{-3}$. An n_{RE} value of 1.53 is assumed.

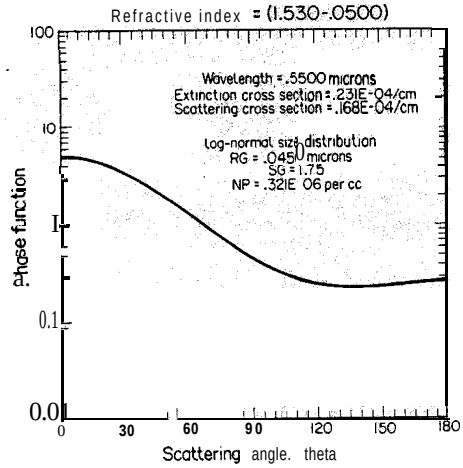

Fig. 3. Scattering phase function for a wavelength of 0.55 μm calculated for smoke emissidns with $n_{IM} = 0.05$. The phase functions for the other eases shown in Table 5 do not differ significantly from the phase function shown here.

combustion. Overall, the major effect of these lower values of n_{IM} inferred from these earlier data sets' would be to decrease the importance of absorption' calculated for smoldering combustion.

Results for σ_S, σ_E and the ratio of σ_S to σ_A, the single, scattering albedo ω for n_{IM} equal to 0.07, 0.011, 0.004 and 0.03 are shown in Table 5. (σ_A may be determined by subtracting σ_S from σ_E, while σ_A/σ_E is just $1 - \omega$.) A phase function for $n_{IM} = 0.05$ is shown in Fig. 3. The phase functions calculated for the other cases shown in Table 5 do not differ significantly from that shown. The ω values calculated for these cases are of particular interest for plume monitoring because they indicate the importance of absorption as it affects total extinction. ω values range from 0.66 for the flaming case to 0.97 for the purely smoldering case; the 'general' case has a value of 0.82. Although the exact numbers will, undoubtedly vary from these nominal values, these data do indicate that under the conditions of flaming combustion approximately 50 % of total extinction will be due to particulate matter absorption, while under purely smoldering conditions, only about 5 % of extinction will be due to absorption. Lower values of n_{IM} would lead to even less absorption during smoldering. We can say, in general, that there are conditions during flaming combustion in which absorption must be considered as a factor in visibility reduction and in which emissions characterizations by scattering alone will be inadequate. Under conditions of smoldering combustion, however, particulate matter absorption, will have only a minor effect on visibility reduction.

Our calculations indicate that the extinction increases by only 26% in going from smoldering to flaming combustion, if the size distribution remains constant. The data in this study and in a number of previous studies show decreases in particulate matter emissions by a factor of 5-10 in the flaming phase relative to the smoldering phase. And so, in terms of visual impact, the increase in the extinction efficiency with increasing absorption will be much less important than the emissions reduction: These data then confirm that, in terms of smoke extinction, the visual impacts of prescribed burns may be reduced by increasing the relative importance of flaming combustion. We have, of course, not considered possible differences in the size distributions in the flaming and smoldering emissions or differences in impact 'due to the color differences in the plumes under these different conditions.

As a further comparison with previous experimental studies, we have calculated mass-scattering ratios at 500 nm for our nominal size distribution for the four emissions cases considered earlier. n_{RE} values were unchanged, while n_{IM} values were modified slightly from the λ = 550nm values because of the slight wavelength shift. Mass concentration is based on an assumed $\rho = 1.3\,\mathrm{g\,cm^{-3}}$. These data, along with inferences derived from a consideration of data by Tangren (1982), are

n_{IM}	$C_m/\sigma_S[\mu\mathrm{g\,m^{-2}}]$	Comments
0.1	3.3×10^5	Flaming dominant
0.022	2.8×10^5	Smoldering dominant
0.011	2.1×10^5	Smoldering only
0.05	3.0×10^5	'General
—	2.8×10^5	Tangren (1982) estimate (near fire)
—	2.0×10^5	Tangren (1982) estimate (aged plume)

These data show that mass concentration/scattering ratios calculated for low absorption cases are consistent with the values inferred for the plume on the ground near the fire. With our assumptions, a match with the well-aged plume data could not be made; reducing the assumed density, however, would allow a match to ahnost any value in the range of observed values. The'data used for these calculationsare certainly not sufficient to allow us to make a definitive match with these experimental observations. If the size distribution that we have used is a reasonable approximation of the actual size distributions in the fires considered by Tangren, however, these data do suggest that the density in these fires is not larger than $1.3\,\mathrm{g\,cm^{-3}}$ and the scattering is eonsistent with the lower absorption characteristic of the smoldering or the 'general' case rather than the higher absorption characteristics of the flaming case. These data also suggest that some of the variation that has been seen in the mass concentration scattering ratios is consistent with differences. expected on the basis of variation in optical properties of the plume particles.

SUMMARY AND CONCLUSIONS

A factorial study designed to study the effects of fuel loading, moisture, and slope for. pine needle fires showed that the specific absorption exhibited a significant dependence on both the fuel loading and the

slope, but not on the moisture. These factorial results have been interpreted physically in terms of the relative importance of flaming and of smoldering combustion.

For those fires in which flaming combustion predominates, B_a values measured at 632.8 nm are near $1\ m^2\ g^{-1}$; for those in which smoldering combustion predominates the B_a values are near $0.16\ m^2\ g^{-1}$. For those fires in which flaming predominated, there was little difference in the measured B_a values during the course of the fire. For those in which smoldering predominated, there was a large differentiation1 in measured B_a values during the course of the fire, with the B_a values decreasing from $\sim 1\ m^2\ g^{-1}$ in the flaming phase to $\sim 0.04\ m^2\ g^{-1}$ in the smoldering phase. The appearance of the filters for these fires changed from black for the flaming phase to light brown for the smoldering phase, reflecting the difference in measured absorption. The live fuel fires showed a B_a value of $0.44\ m^2\ g^{-1}$ at 632.8 nm, somewhat lower than the comparable nine needle fires;

Emission factor data 'for the-particulate matter emissions from this series of fires were consistent with earlier data with the largest emission factors seen in those fires in which smoldering predominated,

A comparison of C_e values determined from our measured absorption with those determined by thermal-optical techniques showed that the two methods were consistent, although the elemental carbon concentrations inferred from the absorption data are systematically lower than those measured by the thermal-optical techniques.

Our measured absorption values and previously measured size distributions and refractive indices were used to calculate the overall radiative effects of these particulates at $\lambda = 550\ nm$ using Mie scattering routines. These calculations indicate that under the conditions of flaming combustion slightly less than 50 % of the extinction will be due to particulate matter absorption, while under purely smoldering conditions, less than 5 % of the extinction will be due to absorption. These data show that there are conditions'in which absorption must be considered as a factor in visibility reduction and in which emissions characterization by scattering alone will be inadequate. Under conditions of smoldering combustion, however, particulate matter absorption will have only a minor effect on visibility reduction. These calculations also show an increased extinction efficiency for the more highly absorbing particles.

We also calculated mass concentration/scattering ratios at $\lambda = 500nm$ for comparison with previous experimental data. For our nominal size distribution and density, the C_m/σ_S ratio decreased from $3.3 \times 10^5\ \mu g\ m^{-2}$ for $n_{IM} = 0.07$ to $2.7 \times 10^5\ \mu g\ m^{-2}$ for $n_{IM} = 0.007$. The values of the ratio calculated for the low absorption cases are generally consistent with previous experimental results, although these calculations suggest that some of the variations seen in measured values of this ratio may be due to differences in the optical properties of the particulate matter.

Acknowledgements-This work was supported by Cooperative Agreement #18-876 between the U.S. Forest Service Southeastern Forest Experiment Station, and the Georgia Institute of Technology. The authors would like to thank H. Gibbs for his support with sampling procedures and data reduction and R. Burgess and J. Harbin for their support of the combustion laboratory operations.

REFERENCES

Bergstrom R. W. (1979) The effect of carbon particles on atmospheric radiation. ***Carbonaceous Particles in the Atmosphere*** (edited by Novakov T.). LBL-9037, CONF-783101, UC1 1, NTIS, Springfield, VA.

Box G., Hunter W. and Hunter J. (197%) ***Statistics for Experimenters.*** John Wiley, New York.

Foster W. W. (1959) Attenuation of light by wood moke. Br. *J. appl. Phys. 10*, 416–420.

Hänel G. and Dlugi R. (1977) Approximation 'for the absorption coefficient of airborne atmospheric aerosol particles in terms of measurable bulk properties. *Tellus* 29, 75–82.

Johnson R. L., Shah J. J., Carv R. A. and Huntziker J. J. (1981) An automated thermal-optical method for the analysis of carbonaceous aerosol. In ***Atmospheric Aerosol: Source/Air Quality Relationships*** (edited by Marcias E. S. and Hopke P. K.). ACS Symposium Series, No. 167.

Koschmeider H, (1924) Theorie der horizontalen Sichtweite. *Beitre. Phys. Atmos.* 12, 33-53.

Lin C. I., Baker M. B. and Charlson R. J. (1973) Absorption coefficient of atmospheric aerosol: a method of measurement. *Appl. Opt. 12*, 1356–1363.

McMahon C. K. (1983) Characteristics of forest fuels, fires and emissions. Paper No. 83-45.1. Presented at 76th Annual Meeting of the Air Pollution Control Association, Atlanta, GA, 19-24 June 1983.

McMahon C. K. and Tsoukalas S. N. (197%) Polynuclear aromatic hydrocarbons in forest fire smoke. In ***Carcinogenesis, Vol. 3: Polynuclear Aromatic Hydrocarbons*** (edited by Jones P. W. and Freudenthal R. I.), pp. 61-73. Raven Press, New York.

Middleton' W. E. K. (1952) ***Vision Through the Atmosphere.*** University of Toronto, Toronto, Canada.

Nolan J. L. (1977) Measurement of light absorbing aerosols for combustion sources. M.S. thesis, University of Washington, Dep. of Civil Engineering.

Nolan J. L. (1979) Measurement of light absorbing aerosols from combustion sources. In ***Carbonaceous Particles in the Atmosphere*** (edited by Novakov T.) LBL-9037, CONF-7803101, UC11, NTIS, Springfield, VA.

Patterson E. M. (1979) Optical properties of urban aerosols containing carbonaceous material. In ***Carbonaceous Particles in the Atmosphere*** (edited by Novakov T.). LBL-9037, CONF-7803101, UC11, NTIS, Springfield, VA.

Patterson E. M., Gillette D. A. and Stockton B. H. (1977) Complex index of refraction between 300 and 700 nm for Saharan aerosols. *J. geophys. Res. 82*, 3153–3160.

Patterson E. M. and McMahon C. K. (1983) Absorption characteristics of forest fire particulate matter. Final Report for U.S. Forest Service Project FS-SE-2110-8(2). On file at Southern Forest Fire Laboratory, Southeastern Forest Experiment Station, Macon, Georgia.

Patterson E. M. and Marshall B. T. (1982) Diffuse reflectance and diffuse transmission measurements of aerosol absorption at the First International Workshop on Light Absorption by Aerosols. *Appl. Opt.* 21, 387–393.

Patterson E. M., Marshall B. T. and Rahn K. A. (1982) Radiative properties of the Arctic aerosol. ***Atmospheric Environment*** *16*, 1967-1977.

Radke L. S., Lyons J. H., Hegg B. A., and Hobbs P. V. (19833 Project Report Lockheed EMSCO Project, A.M. 526 and A.M. 680.

Roessler D. M. and Faxvog F. R. (1981)' Visibility in absorbingaerosols. *Atmospheric Environment* 15, 151–155.

Rosen H., Hansen A. D. A., Gundel L. and Novakov T. (1978) Identification of the graphitic component of source and ambient particulates by Raman spectroscopy and an optical attenuation technique. *Appl. Opt.* 17, 3859-3861.

Russell P. A. (1979) Carbonaceous particulates in the atmosphere: illumination by electron microscopy. In ***Carbonaceous Particles 'in the Atmosphere*** (edited by Novakov T.). LBL-9037, CONF-7803101, UC11, NTIS, Springfield, VA.

Ryan P. W. and McMahon C. K. (1976) Some chemical and physical characteristics of emissions from forest fires. Paper No. 76-2.3, presented at 69th Annual Meeting of the, Air Pollution Control Association, Portland; OR, 22 June-l July 1976.

Sadler M., Charlson R. J., Rosen H. and Novakov T. (1981) An intercomparison of the integrating plate and the laser transmission methods for determination-of aerosol absorption coefficients. *Atmospheric Environment* 15, 1265-1268.

Sandberg D. V., Pierovich J. M., Fox D. G. and Ross E. W. (1978) Effects of fire on aii. USDA Forest Service General Technical Report WO-9, U.S. Government Printing Office, Washington, DC.

Stith J. L., Radke L. F. and Hobbs P. V. (1981) Particle emissions and the production of ozone and nitrogen oxides from the burning of forest slash. *Atmospheric Environment* 15,. 73-82.

Szkarlat A. C. and Japar S. M. (1981) Light absorption by airborne aerosols: comparison of integrating plate and spectrophone techniques. *Appl. Opt. 20,* 1151-1155.

Tangren C. D. (1982) Scattering coefficient and particulate matter concentration in forest fire smoke. ***J. Air Pollut. Control Ass. 32, 729-732.***

Ward D. E., Elliott E. R., McMahon C. K. and Wade D. D. (1976) Particulate source strength determination for low-intensity prescribed fires. ***Proc. Control Technology of Agricultural Air Pollutants Specialty Conference,*** Air Pollution Control Association, Pittsburgh, PA, March 1974, 39–55.

Weiss R. E., Charlson R. J., Waggoner A. P., Baker M. B., Covert D., Thorsell D. L. and Yuen S. (1976) Applications of directly measured aerosol radiative properties to climate models. Atmospheric aerosols: their optical properties and effects. NASA CP 2004, available from NTIS, Springfield, VA.

Weiss R. E., Waggoner A. P., Charlson R. J., Thorsell D. L., Hall J. C. and Riley L. S. (1979) Studies of the optical, physical and chemical properties of light absorbing aerosols. In *Carbonaceous Particles in the Atmosphere* (edited by Novakov T.). LBL-9037, CONF-783101, UC11, NTIS, Springfield, VA.